Carbohydrate Polymers 87 (2012) 2086–2092

Contents lists available at SciVerse ScienceDirect

Carbohydrate Polymers

journal homepage: www.elsevier.com/locate/carbpol

# Structural characterisation of oligosaccharides obtained by Fenton-type radical depolymerisation of dermatan sulfate

Charalambos Panagos[a], Derek Thomson[b], Charles D. Bavington[b], Dušan Uhrín[a,*]

[a] EaStCHEM School of Chemistry, Joseph Black Building, The King's Buildings, Edinburgh, EH9 3JJ, UK
[b] GlycoMar Ltd, European Centre for Marine Biotechnology, Oban, Scotland, PA37 1QA, UK

ARTICLE INFO

*Article history:*
Received 20 August 2011
Received in revised form 8 October 2011
Accepted 14 October 2011
Available online 20 October 2011

*Keywords:*
Dermatan sulfate
Glycosaminoglycans
Fenton radical depolymerisation
NMR

ABSTRACT

The contamination of heparin in 2008 brought to the attention of health authorities an urgent need for structural characterisation of low molecular weight heparins and other glycosaminoglycans (GAGs) intended for clinical applications. Potentially harmful compounds can be introduced into these preparations as contaminants of the original material or as by-products of the depolymerisation process. Radical depolymerisation is one of the methods used for fractionations of GAGs. We report here on the results of the Fenton-type radical depolymerisation of dermatan sulfate (DS) by hydrogen peroxide in the presence of $Cu^{2+}$ cations. A low molecular fraction of the reaction mixture was investigated by a combination of 2D $^{1}H$,$^{13}C$ HSQC, 2D HSQC-TOCSY and 2D HMBC experiments at 800 MHz. The analysis of the spectra revealed the formation of oligosaccharides with structures corresponding to the native DS sequence and containing almost exclusively GalNAc4S as the reducing end monosaccharide. In addition, oligosaccharides containing a C-4 sulfated N-acetylgalactosaminic acid in place of the reducing end GalNAc4S were identified. This open chain monosaccharide represents a non-native DS structure.



## 1. Introduction

Glycosaminoglycans (GAGs) are a group of structurally related polysaccharides found in living organisms as free polysaccharides and as the carbohydrate moieties of proteoglycans. They are widely distributed throughout the animal kingdom (Cássaro & Dietrich, 1977; Mathews, 1975; Medeiros et al., 2000) and are essential for maintaining the structural integrity of many connective tissues (Comper & Laurent, 1978). They also exert important regulatory functions through binding to numerous proteins, including chemokines, cytokines, defensins, growth factors, morphogens, enzymes, proteins of the complement system and of the extracellular matrix (Imberty, Lortat-Jacob, & Pérez, 2007).

Different types of GAGs are distinguished by their monomeric composition, position and configuration of their glycosidic linkages and by the amount and location of their sulfate substituents (Lindahl & Höök, 1978). The most prominent member of the GAG family is heparin. Exogenous heparin has profound effects on the coagulation system due to heparin's ability to bind antithrombin and heparin cofactor II and is currently used as an anticoagulant and antithrombotic drug (Guerrini, Naggi, Guglieri, Santarsiero, & Torri, 2005). Unfractionated heparin is known to cause undesirable side effect such as heparin-induced thrombocytopenia (Fabris et al., 2000). Low molecular weight heparins (LMWHs) prepared by chemical or enzymatic depolymerisation of heparin (Linhardt et al., 1990) are used throughout the world as improved antithrombotic/anticoagulant agents. LMWH has also found use in other medicinal applications (Castelli, Porro, & Tarsia, 2004).

Dermatan sulfate, DS, another member of the GAG family, plays an important role in cell growth, differentiation, morphogenesis, migration and bacterial/viral infections (Volpi, 2010). Although the clinical use of DS is presently limited, its numerous biological activities make it a potential candidate for the development of DS-based therapeutics (Linhardt & Hileman, 1995; Volpi, 2010). DS exhibits anticoagulant activity (Liaw, Becker, Stafford, Fredenburgh, & Weitz, 2001) and low molecular weight dermatan sulfates (LMWDS) prepared by radical depolymerisation of DS (Mascellani, Liverani, Parma, Bergonzini, & Bianchini, 1996) have been shown to increase bioavailability without the loss of bioactivity (Legnani et al., 1994).

As illustrated by these two examples, low molecular weight GAGs are viable alternatives to their parent polysaccharide species

*Abbreviations:* GAGs, glycosaminoglycans; LMWH, low molecular weight heparin; DS, dermatan sulfate; GalNAc4S, N-acetylgalactosamine; IdoA, iduronic Acid; ΔU, $\Delta^{4,5}$ unsaturated uronic acid; HSQC, Heteronuclear single quantum coherence; TOCSY, Total correlation spectroscopy; HMBC, Heteronuclear multiple bond coherence; DIPSI, decoupling in the presence of scalar interactions.

* Corresponding author. Tel.: +44 1316507061; fax: +44 1316507155.
*E-mail addresses:* c.panagos@sms.ed.ac.uk (C. Panagos), derek@glycomar.com (D. Thomson), charlie@glycomar.com (C.D. Bavington), dusan.uhrin@ed.ac.uk (D. Uhrín).

0144-8617/$ – see front matter © 2011 Elsevier Ltd. All rights reserved.
doi:10.1016/j.carbpol.2011.10.031

for pharmaceutical applications. The methods of preparation of low molecular weight GAGs vary (Linhardt & Gunay, 1999; Linhardt et al., 1990; Ofman, Slim, Watt, & Yorke, 1997; Volpi, Mascellani, & Bianchini, 1992). One of the depolymerisation methods is the free radical depolymerisation. However, the mechanism and products of the radical depolymerisation procedures are still not fully understood and characterised.

Depolymerisation of GAGs is also a useful tool in the structural characterisation of unknown GAGs. For example, structure determination of GAGs isolated from marine invertebrae is challenging due to their structural heterogeneity. (Chen et al., 2011; Mourão et al., 1996; Pavão, Mourão, Mulloy, & Tollefsen, 1995; Vieira, Mulloy, & Mourão, 1991). However, marine GAGs are usually resistant to enzymatic depolymerisation (Vieira et al., 1991); chemical depolymerisation could therefore help to unravel their structures, as well as help with the identification of functionally important patterns in their sequences (Pavão et al., 1995).

Radical depolymerisation has been applied to GAGs, such as heparin (Nagasawa, Uchiyama, Sato, & Hatano, 1992), chondroitin sulfate, dermatan sulfate (Ofman et al., 1997), hyaluronate (Uchiyama, Dobashi, Ohkouchi, & Nagasawa, 1990) and marine GAGs (Wu, Xu, Zhao, Kang, & Ding, 2010b). Recently, the products and the mechanism of partial $Cu^{2+}$ and $Fe^{2+}$ Fenton-type depolymerisation of heparin (Vismara et al., 2007, 2010) have been investigated.

Here we present structural analysis of oligosaccharides obtained by $Cu^{2+}$ catalyzed Fenton-type depolymerisation of DS. Our aim is to investigate the specificity of the cleavage and to characterise any non-native structures that may result from the depolymerisation process. The oligosaccharides, partially separated by size exclusion chromatography, were characterised by 2D $^{1}H$–$^{13}C$ heterocorrelated NMR spectroscopy and compared to those obtained by the enzymatic cleavage of DS. We also demonstrate that NMR spectroscopy at high magnetic fields is able to analyse complex mixtures of related GAG oligosaccharides without the need for complete separation.

## 2. Materials and methods

### 2.1. Materials

Porcine DS, composed almost exclusively from the repeating disaccharide [-β-D-GalNAc4S-(1 → 4)-α-L-IdoA-(1 → 3)-]$_n$ was obtained from Celsus Laboratories. Chondroitinase B was purchased from Grampian Enzymes. Ethylenediaminetetraacetic acid (EDTA) and trimethylsilyl propionate (TSP) were purchased from Goss Scientific Instruments Ltd. and Aldrich, respectively. Sigma–Aldrich Chelex (C7901) was used.

### 2.2. Free radical depolymerisation of DS

DS (2 g) was dissolved in 1 L of $H_2O$ and the vessel was heated to 55 °C. $CuSO_4$ (1.6 g) was added to yield a final concentration of 0.01 M $Cu^{2+}$. The pH was adjusted to 7.5 using 1 M NaOH. The $H_3O^+$ ions released during the reaction were neutralized by adding small amounts of 0.1 M NaOH and pH was re-adjusted to 7.5 every 5 min. Samples were taken every 15 min and analysed by HPLC SEC (YMC Diol 60, RI detection), in order to monitor the progress of the reaction. After 90 min the pH became stable at which point the reaction was stopped by adding acetic acid (5 μl/ml, 20%). The free copper ions were partially removed by adding Chelex (60 mg/ml) and the supernatant was decanted. The remaining free and associated $Cu^{2+}$ ions were exchanged by passing the decanted solution through an anion exchange Q-Sepharose column (GE Healthcare) using 50 mM NaCl as the running buffer. The bound oligosaccharides were eluted using a 2 M NaCl buffer. The oligosaccharides were desalted and fractionated using a Buchi Sepacore Chromatography system equipped with a Superdex 30 size exclusion column (GE Healthcare). The molecular size of oligosaccharides in each fraction produced was estimated using a HPLC system with RI detection (Waters) equipped with a YMC Diol 60 column (Crawford Scientific) calibrated with heparin oligosaccharide standards (Iduron). The three lowest molecular weight fractions, subsequently labelled **I–III**, contained 41.7 mg, 19.9 mg and 6.9 mg of oligosaccharides.

### 2.3. Enzymatic depolymerisation of DS

DS (100 mg) was dissolved in Tris buffer (50 ml, 50 mM Tris, 3 mM $CaCl_2$, 50 mM NaCl at pH 7.5). Initially, chondroitinase B (0.4 units) was added but enzymatic digestion was observed to be poor, likely due to the presence of proteases in the reaction mixture. After the addition of BSA (0.5 mg/ml) and a further 0.2 units of chondroitinase B the digestion improved. The digestion was monitored by injecting 5–20 μl aliquots of the reaction mixture on a Superdex Peptide 10/300GL (GE Healthcare) column attached to a Waters 600 LCD HPLC with a 486 Tunable Absorbance Detector tuned to 232 nm. The flow rate was 0.5 ml/min and a PBS buffer (100 mM) was used as the mobile phase. The reaction was stopped after 72 h and the sample freeze dried. The freeze dried material was dissolved in doubly distilled water (2 ml) and size fractionized on a 2*XK26 column (GE Healthcare) packed with BioGel P10 fine resin (BioRad). The flow rate was adjusted to 0.4 ml/min and 5 ml fractions were collected. The disaccharide and tetrasaccharide fractions were freeze dried and re-dissolved in 1 ml of $dH_2O$.

### 2.4. NMR spectroscopy

The samples were desalted prior to NMR experiments on a 1.6 × 30 GE Healthcare Sephadex G-25 superfine column on a BioCAD FPLC system using $dH_2O$ as a running buffer. After lyophilisation the samples were dissolved in 99.9% $D_2O$, (Aldrich, 540 μl) containing deuterated $NaH_2PO_4 + HNa_2HPO_4$ buffer (10 mM, pH 7.2). A stock solution (20 μl) of EDTA and TSP was added. The stock solution was prepared by dissolving EDTA (4 mg) and TSP (9 mg) in the phosphate buffer (200 μl). The pH was adjusted to 7.2 by adding few drops of a concentrated solution of NaOH in $D_2O$. All spectra were acquired at 50 °C on an 800 MHz Avance I Bruker NMR spectrometer equipped with a z-gradient triple-resonance TCI cryoprobe. The spectra were referenced (0 ppm) using the $^{1}H$ and $^{13}C$ signals of TSP.

1D $^{13}C$ NMR spectra were acquired using relaxation and acquisition times of 1.5 and 0.185 s, respectively; 40,960 scans per spectrum were accumulated in 20 h. The FIDs were zero filled once and a 2 Hz exponential line broadening was applied prior to Fourier transformation. 2D $^{1}H$,$^{13}C$ HSQC spectra were acquired using $t_1$ and $t_2$ acquisition times of 19.9 and 53 ms, respectively; 8 scans were acquired into each of 400 $F_1$ complex data points resulting in the total experimental times of 2.5 h per sample. The standard 2D HSQC-TOCSY BRUKER pulse sequence was modified by appending a $^{1}H$ spin-echo of overall duration of $1/^{1}J_{CH}$ (optimized for a $^{1}J_{CH}$ = 150 Hz) after the TOCSY spin-lock and two 2D $^{1}H$,$^{13}C$ HSQC-TOCSY spectra were acquired in an interleaved manner. The first one with and the second one without a 180° $^{13}C$ pulse applied simultaneously with the 180° $^{1}H$ pulse of the final spin-echo. This resulted in a difference in sign of one-bond cross peaks between the two spectra. Addition of the two 2D matrices prior to processing yielded a 2D HSQC-TOCSY spectrum with substantially reduced one-bond crosses peaks. Such treatment has facilitated identification of weak TOCSY cross peaks. The subtraction of matrices yielded a $^{1}H$,$^{13}C$ HSQC spectrum. Each 2D HSQC-TOCSY spectrum was acquired using $t_1$ and $t_2$ acquisition times of 51 and 106 ms, respectively; 1024 complex data points using 4 scans were collected in $F_1$

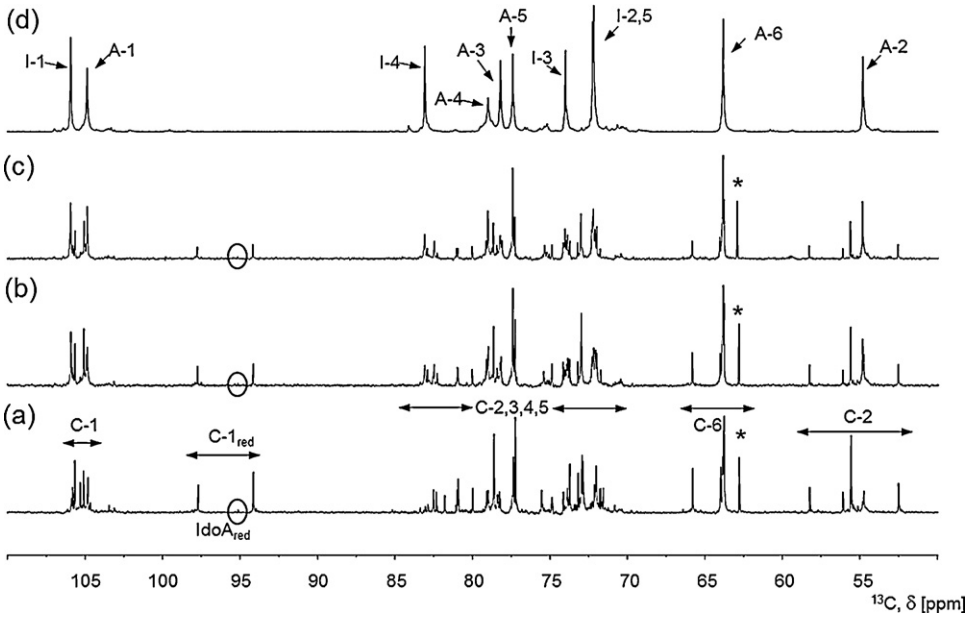


**Fig. 1.** Partial $^{13}$C NMR spectra (a)–(c) of fractions **I**–**III** obtained by size exclusion chromatography and a partial $^{13}$C NMR spectrum (d) of unfractionated DS. The circled signals belong to the anomeric carbon of the reducing IdoA. Signals denoted by an asterisk belong to a small molecular impurity.

in each experiment; the total duration of the experiment was 7 h. A DIPSI-2 mixing sequence was applied for 20 or 60 ms. 2D $^{1}$H–$^{13}$C HMBC spectra (Cicero, Barbato, & Bazzo, 2001) were acquired using $t_1$ and $t_2$ acquisition times of 14 and 367 ms, respectively; 1024 complex data points were collected in $F_1$; the total duration of the experiment was 7.5 h. The experiment was optimized for the $^{n}J_{CH}$ of 6 Hz and a two-stage one-bond correlation filter was set for $^{1}J_{CH}$ of 120 (minimum) and 160 (maximum) Hz.

## 3. Results

### 3.1. Structural analysis of oligosaccharides obtained by the free radical depolymerisation of DS

The three low molecular weight oligosaccharide fractions, **I**–**III**, obtained by the Fenton-type depolymerisation of DS, as detailed in the Materials and Methods, were investigated by NMR. Their $^{13}$C NMR spectra (Fig. 1) indicate an increased oligosaccharide length from fraction **I** to **III** as implied from the increasing intensity of signals corresponding to those of the DS polysaccharide. Fraction **I**, containing smallest oligosaccharides, was taken forward for full structural characterisation by NMR.

The inspection of $^{1}$H and $^{13}$C spectra of fraction **I** indicate the presence of several major species. However, the structure elucidation without further separation of individual oligosaccharides was possible using $^{1}$H–$^{13}$C heterocorrelated 2D NMR spectroscopy at 800 MHz and no further attempts were made to separate them. As detailed below, a combination of 2D $^{1}$H,$^{13}$C HSQC, 2D HSQC-TOCSY and 2D HMBC experiments identified two trisaccharides (**1** and **2**) and one tetrasaccharide (**3**) as the main components of fraction **I** (Fig. 2). Oligosaccharides **1** and **3** show anomeric equilibrium at the reducing GalNAc4S. High population of both anomeric forms (56% of α- and 44% of the β-form) added to the complexity of the spectra. The analysis of the spectra showed that the trisaccharide **2** contains at its reducing end a modified GalNAc4S residue.

$^{1}$H spectra of fraction **I** are too complex to yield unambiguous assignment of resonances based on homonuclear experiments. Taking an advantage of a larger dispersion of $^{13}$C chemical shifts, individual spin-systems of GalNAc4S and IdoA rings were identified using a combination of 2D $^{1}$H,$^{13}$C HSQC and 2D HSQC-TOCSY spectra. During a short TOCSY mixing time (~20 ms) of the 2D HSQC-TOCSY experiment, the magnetization is transferred only between geminal or vicinal protons. This minimizes the signal overlap, allowing unambiguous assignment of $^{1}$H and $^{13}$C resonances. The procedure is illustrated in Fig. 3 for residue **A** of tetrasaccharide **3**$^{\alpha}$. Due to a small $^{3}J_{H\text{-}4,H\text{-}5}$ coupling constant, no TOCSY transfer occurs between H-4 and H-5 of galactose residues. The $^{1}$H and $^{13}$C resonances at positions 1–4 of GalNAc4S were therefore linked to those at positions 5 and 6 through long-range proton-carbon couplings of C-4 using the 2D $^{1}$H, $^{13}$C HMBC experiment. Carbon C-4 couples to protons H-3, H-5, H-6a, b (Fig. 3), yielding complete resonance assignment of the GalNAc4S resonances. On the other hand, a complete resonance assignment of IdoA residues was possible solely through the interpretation of 2D $^{1}$H,$^{13}$C HSQC and 2D HSQC-TOCSY spectra. Sets of resonances belonging to individual GalNAc4S and IdoA rings were then connected together using the inter-ring proton-carbon correlations identified in the 2D HMBC spectra (Fig. 4). Cross peaks due to both $^{3}J_{H1,Cx}$ and $^{3}J_{Hx,C1}$ were observed. The procedures outlined above allowed the identification of the structures shown in Fig. 2.

Oligosaccharides **1** and **3** represent regular DS structures with GalNAc as the reducing monosaccharide. However, this is not the case for trisaccharide **2**, which does not show connectivity of the H-2 (4.48 ppm) to the anomeric proton of the reducing GalNAc4S residue. In addition, the corresponding N-acetylated carbon C-2 displays an unusually high $^{13}$C chemical shift (58.24 ppm). In order to establish the structure of this monosaccharide and starting from the H-2 proton, the proton–proton connectivities were traced out all the way to H-6, including the H-4, H-5 connectivity. This indicates that the $^{3}J_{H\text{-}4,H\text{-}5}$ has increased in this species. The resonance assignment was further supported by a familiar pattern of long-range cross peaks of C-4 (to protons H-3, H-5 and H-6) and a long-range coupling of C-3 to the anomeric proton of the preceding IdoA residues. The H-2 proton showed long-range correlation to two carbonyl carbons at 176.6 and 179.3 ppm (data not shown). The former belongs to the NAc carbonyl of the GalNAc4S, while the latter was assigned to an extra carboxylic acid group that resulted from the oxidation of the anomeric carbon. The high chemical shift of C-4 (80.92) indicates that this position is sulfated. The above

**DS** [-β-D-GalNAc4S-(1→4)-α-L-IdoA-(1→3)-]$_n$

**1** β-D-GalNAc4S-(1→4)-α-L-IdoA-(1→3)-α/β-D-GalNAc4S
C B C B A

**2** β-D-GalNAc4S -(1→4)-α-L-IdoA-(1→3)-R
C B A

**3** α-L-IdoA-(1→3)-β-D-GalNAc4S-(1→4)-α-L-IdoA-(1→3)-α/β-D-GalNAc4S
D C B A

**4** ΔU-(1→3)-β-D-GalNAc4S -(1→4)-α-L-IdoA-(1→3)-α/β-D-GalNAc4S
D C B A

**5** ΔU-(1→3)-α/β-D-GalNAc4S
D A

R=

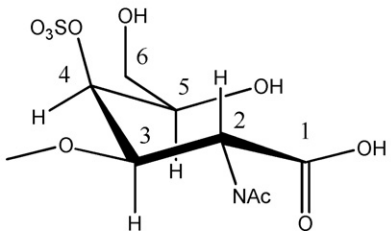


**Fig. 2.** Oligosaccharides produced by the radical depolymerisation (**1**–**3**) or enzymatic digestion (**4** and **5**) of **DS**.

analysis shows that trisaccharide **2** contains a C-4 sulfated acetylgalactosaminic acid at its reducing end.

2D $^{1}$H,$^{13}$C HSQC spectra of fractions **II** and **III** (data not shown) confirmed that these fractions also contain acetylgalactosaminic acid. We assume that the acetylgalactosaminic acid is present here as part of tetra- and higher oligosaccharides. Due to the open ring structure, the tetrasaccharide containing acetylgalactosaminic acid behaves as a bigger molecule than tetrasaccharide **3** on the size exclusion column HPLC SEC and therefore is not present in fraction **I**.

The assignment of $^{1}$H and $^{13}$C resonances of oligosaccharides **1**–**3** was verified by comparing their chemical shifts with those of the enzymatically prepared tetrasaccharide **4** and disaccharide **5**. The resonances of the latter species were assigned using the same procedure as employed for the resonance assignment of oligosaccharides **1**–**3**. A very good agreement was observed for rings A–C between the tetrasaccharides **4** and **3** and rings A and B of **4** and those of the trisaccharide **2**. The $^{1}$H and $^{13}$C chemical shifts of the inner **B** and **C** rings of tetrasaccharides **3** are also in excellent agreement with those of **DS** (Table 1).

## 4. Discussion

The low molecular fraction **I** obtained by the $Cu^{2+}$ catalyzed Fenton depolymerisation of DS contains trisaccharides **1** and **2** and a tetrasaccharide **3**. Oligosaccharides **1** and **3** have regular DS

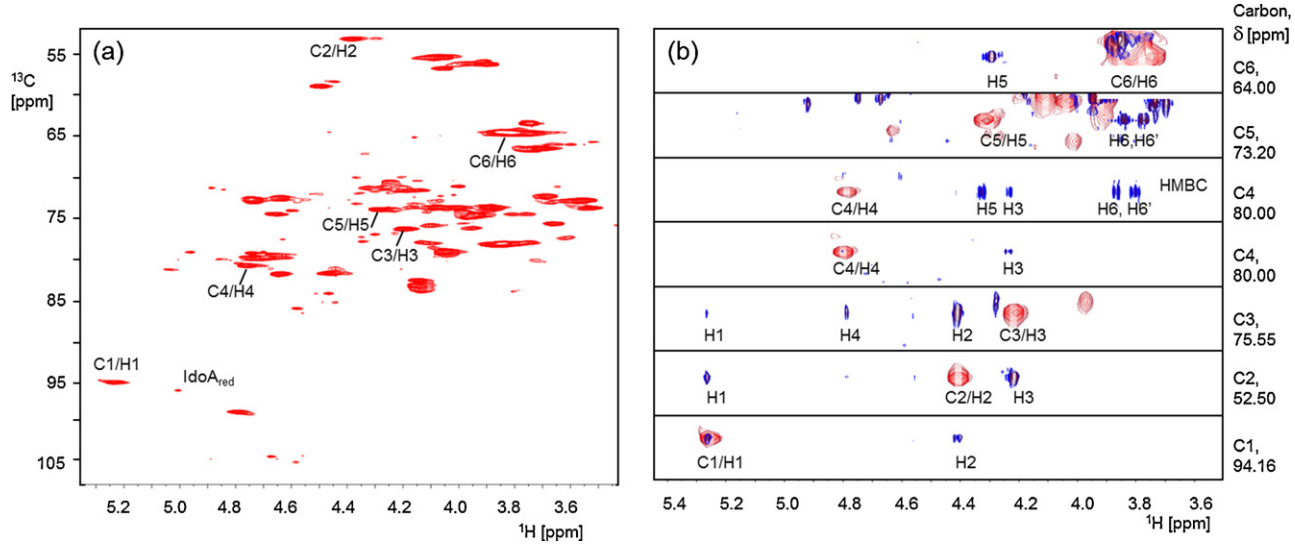


**Fig. 3.** (a) 2D $^{1}$H,$^{13}$C HSQC spectrum of fraction **I**. Cross peaks of the of the residue **A** of tetrasaccharide **3**$^{\alpha}$ are labelled; (b) $F_2$ slices through C-1 to C-6 carbon resonances of residue **A** in tetrasaccharide **3**$^{\alpha}$ taken from 2D $^{1}$H,$^{13}$C HSQC (grey), 2D HSQC-TOCSY (black) and 2D HMBC (C4, black) spectra of fraction **I**.

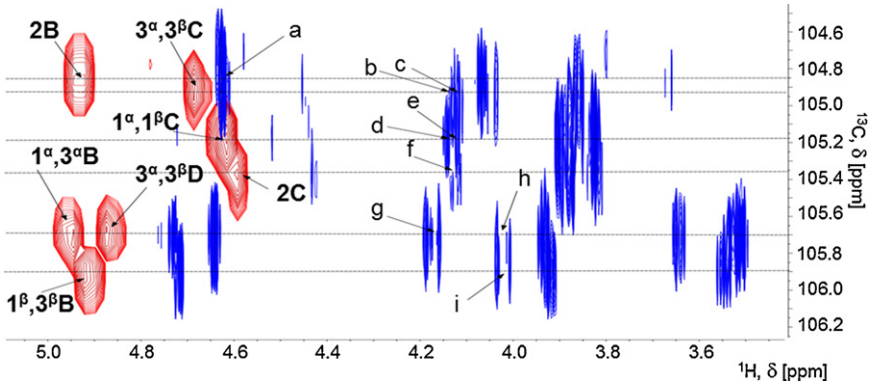


**Fig. 4.** Overlay of the anomeric region of the 2D $^{1}H,^{13}C$ HSQC (grey) and 2D HMBC (black) spectra of mixture **I**. Only the one-bond correlation (HSQC) and interglycosidic (HMBC) cross peaks are assigned. HMBC peaks are annotated **a**–**i**, according to the following key; **a** = 2B C1 → H3 2R, **b** = $3^{\alpha}$C C1 → H4 $3^{\alpha}$B, **c** = $3^{\beta}$C C1 → H4 $3^{\beta}$B, **d** = $1^{\alpha}$C C1 → H4 $1^{\alpha}$B, **e** = $1^{\beta}$C C1 → H4 $1^{\beta}$B, **f** = 2 C C1 → H4 2B, **g** = $1^{\alpha},3^{\alpha}$B C1 → H3 $1^{\alpha},3^{\alpha}$A, **h** = $3^{\alpha},3^{\beta}$D C1 → H3 $3^{\alpha},3^{\beta}$C, **i** = $1^{\beta},3^{\beta}$B C1 → H3 $1^{\beta},3^{\beta}$A.

structures with GalNAc4S as the reducing end residue. The absence of the reducing IdoA residue is very notable; only very weak, additional signals were observed in the reducing monosaccharide region of the 1D $^{13}C$ (Fig. 1) and 2D $^{1}H,^{13}C$ HSQC spectra (see Fig. 3 for fraction **I**) of all fractions. These HSQC peaks, assigned to α-IdoA and β-IdoA residues, appear at 5.11/97.52 and 4.99/95.15 ppm, respectively. In the 1D $^{1}H$ and $^{13}C$ spectra of fraction **I**, the β-IdoA signal is barely visible, whereas the α-IdoA signal is lost in the noise.

The lack of any substantial amount of reducing end IdoA residue cannot be used to suggest that the depolymerisation reaction does not cleave the -3)α-L-IdoA-(1 → 3)-β-D-GalNAc4S-(1-glycosidic linkage. The very existence of trisaccharides **1** and **2** contradicts this suggestion; this trisaccharide contains a non-reducing GalNAc4S residue, implying that this IdoA-(1 → 3)-β-D-GalNAc4S linkage was broken.

It has been reported previously that the unsulfated IdoA is preferentially degraded by the free radical depolymerisation of

**Table 1**
$^{1}H$ and $^{13}C$ chemical shifts of DS and oligosaccharides 1–5.[a]

| Compound | Residue | $^{1}H$ chemical shifts[b] (ppm) | | | | | | | $^{13}C$ chemical shifts[b] (ppm) | | | | | | | |
|---|---|---|---|---|---|---|---|---|---|---|---|---|---|---|---|---|
| | | H-1 | H-2 | H-3 | H-4 | H-5 | H-6 | CH3 | C-1 | C-2 | C-3 | C-4 | C-5 | C-6 | CH3 | NAc |
| **DS** | **B** -4)-α-L-IdoA-(1- | 4.90 | 3.54 | 3.91 | 4.11 | 4.72 | – | – | 105.96 | 72.2 | 74.00 | 83.07 | 72.29 | 176.68 | – | – |
| | **C** -3)-β-D-GalNAc4S-(1- | 4.68 | 4.04 | 4.02 | 4.68 | 3.85 | 3.80 | 2.08 | 104.91 | 54.84 | 78.26 | 78.98 | 77.45 | 63.86 | 25.44 | 177.91 |
| **$1^{\alpha}$** | **A** -3)-α-D-GalNAc4S | 5.13 | 4.37 | 4.17 | 4.74 | 4.27 | 3.73–3.8 | 2.066 | 94.16 | 52.50 | 75.55 | 80.00 | 73.20 | 64.00 | 24.93 | 177.35 |
| | **B** -4)-α-L-IdoA-(1- | 4.95 | 3.53 | 3.94 | 4.14 | 4.73 | – | – | 105.68 | 72.03 | 73.73 | 82.35 | 71.81 | 176.75 | – | – |
| | **C** β-D-GalNAc4S-(1- | 4.62 | 3.88 | 3.87 | 4.69 | 3.83 | 3.82 | 2.08 | 105.12 | 55.56 | 72.92 | 78.63 | 77.24 | 63.81 | 25.44 | 178.10 |
| **$1^{\beta}$** | **A** -3)-β-D-GalNAc4S | 4.78 | 4.04 | 4.03 | 4.67 | 3.85 | 3.83 | 2.066 | 97.72 | 56.09 | 78.27 | 79.01 | 77.38 | 63.77 | 24.93 | 177.92 |
| | **B** -4)-α-L-IdoA-(1- | 4.91 | 3.55 | 3.92 | 4.13 | 4.72 | – | – | 105.85 | 72.13 | 73.87 | 72.02 | 72.02 | 176.68 | – | – |
| | **C** β-D-GalNAc4S-(1- | 4.62 | 3.88 | 3.87 | 4.69 | 3.83 | 3.82 | 2.08 | 105.12 | 55.56 | 72.92 | 78.63 | 77.24 | 63.81 | 25.44 | 178.10 |
| **2** | **R** | – | 4.48 | 4.62 | 4.45 | 3.99 | 3.69 | 2.069 | 176.56 | 58.24 | 81.00 | 80.92 | 72.98 | 65.78 | 25.09 | 179.28 |
| | **B** -4)-α-L-IdoA-(1- | 4.94 | 3.67 | 4.07 | 4.13 | 4.62 | – | – | 104.81 | 71.56 | 72.91 | 81.78 | 71.72 | 176.82 | – | – |
| | **C** β-D-GalNAc4S-(1- | 4.60 | 3.88 | 3.87 | 4.69 | 3.83 | 3.82 | 2.08 | 105.34 | 55.57 | 72.92 | 78.63 | 77.24 | 63.81 | 25.44 | 178.14 |
| **$3^{\alpha}$** | **A** -3)-α-D-GalNAc4S | 5.22 | 4.37 | 4.17 | 4.74 | 4.27 | 3.72–3.8 | 2.066 | 94.16 | 52.50 | 75.55 | 80.00 | 73.20 | 64.00 | 24.93 | 177.35 |
| | **B** -4)-α-L-IdoA-(1- | 4.95 | 3.53 | 3.94 | 4.13 | 4.73 | – | – | 105.68 | 72.03 | 73.73 | 82.91 | 71.81 | 176.75 | – | – |
| | **C** -3)-β-D-GalNAc4S-(1- | 4.68 | 4.12 | 4.03 | 4.70 | 3.85 | 3.83 | 2.08 | 104.9 | 54.76 | 78.45 | 79.10 | 77.38 | 63.77 | 25.44 | 177.60 |
| | **D** α-L-IdoA-(1- | 4.87 | 3.51 | 3.65 | 3.96 | 4.64 | – | – | 105.68 | 73.00 | 74.90 | 74.16 | 73.75 | 178.47 | – | – |
| **$3^{\beta}$** | **A** -3)-β-D-GalNAc4S | 4.78 | 4.04 | 4.03 | 4.67 | 3.85 | 3.83 | 2.066 | 97.72 | 56.09 | 78.27 | 79.01 | 77.38 | 63.77 | 24.93 | 177.92 |
| | **B** -4)-α-L-IdoA-(1- | 4.91 | 3.55 | 3.92 | 4.12 | 4.72 | – | – | 105.85 | 72.13 | 73.87 | 83.03 | 72.02 | 176.68 | – | – |
| | **C** -3)-β-D-GalNAc4S-(1- | 4.68 | 4.12 | 4.03 | 4.70 | 3.85 | 3.83 | 2.08 | 104.90 | 54.76 | 78.45 | 79.10 | 77.38 | 63.77 | 25.44 | 177.60 |
| | **D** α-L-IdoA-(1- | 4.87 | 3.51 | 3.65 | 3.96 | 4.64 | – | – | 105.68 | 73.00 | 74.90 | 74.16 | 73.75 | 178.47 | – | – |
| **$4^{\alpha}$** | **A** -3)-α-D-GalNAc4S | 5.21 | 4.36 | 4.18 | 4.74 | 4.27 | 3.72–3.79 | 2.057 | 94.94 | 52.68 | 75.57 | 80.20 | 73.38 | 64.19 | 24.92 | 177.37 |
| | **B** -4)-α-L-IdoA-(1- | 4.94 | 3.54 | 3.93 | 4.13 | 4.73 | – | – | 105.87 | 72.39 | 74.12 | 83.14 | 72.31 | 176.69 | – | – |
| | **C** -3)-β-D-GalNAc4S-(1- | 4.70 | 4.06 | 4.16 | 4.631 | 3.86 | 3.79 | 2.12 | 104.98 | 55.04 | 78.51 | 79.16 | 77.56 | 63.94 | 25.45 | 177.87 |
| | **D**[c] ΔU | 5.26 | 3.84 | 3.95 | 5.95 | – | – | – | 103.06 | 71.66 | 67.62 | 109.48 | 147.19 | 171.95 | – | – |
| **$4^{\beta}$** | **A** -3)-β-D-GalNAc4S | 4.77 | 4.03 | 4.03 | 4.68 | 3.84 | 3.77–3.79 | 2.057 | 97.92 | 56.25 | 78.30 | 79.22 | 77.55 | 64.06 | 25.09 | 177.61 |
| | **B** -4)-α-L-IdoA-(1- | 4.90 | 3.55 | 3.92 | 4.12 | 4.72 | – | – | 106.02 | 72.49 | 74.28 | 83.32 | 72.52 | 176.77 | – | – |
| | **C** -3)-β-D-GalNAc4S-(1- | 4.70 | 4.06 | 4.16 | 4.63 | 3.86 | 3.79 | 2.12 | 104.98 | 55.04 | 78.51 | 79.16 | 77.56 | 63.94 | 25.45 | 177.87 |
| | **D**[c] ΔU | 5.26 | 3.84 | 3.95 | 5.95 | – | – | – | 103.06 | 71.66 | 67.62 | 109.48 | 147.19 | 171.95 | – | – |
| **$5^{\alpha}$** | **A** -3)-α-D-GalNAc4S | 5.22 | 4.38 | 4.31 | 4.70 | 4.27 | 3.71–3.78 | 2.09 | 94.11 | 52.60 | 75.60 | 80.02 | 73.28 | 63.98 | 24.90 | 177.21 |
| | **D**[c] ΔU | 5.30 | 3.85 | 3.96 | 5.96 | – | – | – | 102.75 | 71.53 | 67.51 | 109.33 | 147.01 | 171.91 | – | – |
| **$5^{\beta}$** | **A** -3)-β-D-GalNAc4S | 4.79 | 4.06 | 4.18 | 4.63 | 3.85 | 3.75 | 2.09 | 97.72 | 56.20 | 78.10 | 78.98 | 77.40 | 63.85 | 25.07 | 177.47 |
| | **D**[c] ΔU | 5.26 | 3.85 | 3.96 | 5.96 | – | – | – | 102.71 | 71.53 | 67.51 | 109.33 | 147.01 | 171.96 | – | – |

[a] See Fig. 2 for the structures.
[b] Relative to TSP, 0 ppm.
[c] ΔU–$\Delta^{4,5}$-uronic acid.

both heparin (Nagasawa et al., 1992) and DS (Ofman et al., 1997) and selectively oxidized to volatile acids (i.e. formic acid) (Linhardt & Gunay, 1999). Supporting this last suggestion, more recent studies of Fenton depolymerisation of heparin (Vismara et al., 2007, 2010) established the reduced occurrence of the -4)α-L-IdoA-(1 → 4)-α-D-Glc(NS/NAc)-(1-disaccharide amongst the depolymerised products. However, the reducing IdoA residue was not detected. The authors only observed IdoA2S as the reducing residue suggesting that (i) the Fenton depolymerisation indeed cleaves the glycosidic linkage between an uronic acid and a hexosamine, and (ii) that the proposed oxidation of the uronic acid is only taking place in the absence of C-2 sulfation. Most of the reducing end IdoA produced by the depolymerisation of DS is therefore lost by radical degradation, which explains its almost complete absence as the reducing end sugar. Free radical depolymerisation of heparin (Vismara et al., 2007, 2010) also showed the resistance of the -4)α-L-IdoA-(1 → 4)-α-D-Glc(NS/NAc)6S-(1-disaccharide towards the cleavage by radicals indicating a protective role of the C-6 sulfation of the hexosamine. This observation is consistent with our DS data. The main sulfation pattern of DS, one sulfate group per disaccharide repeating unit at GalNAc4S, allows for the degradation of the preceding non-sulfated IdoA. As a consequence the main oligosaccharides produced contain GalNAc4S residues at their reducing end.

In addition to the unmodified DS oligosaccharides, we have also characterised trisaccharide **2**, in which the reducing GalNAc4S ring was oxidized forming the acetylgalactosaminic acid. This moiety was also present in the higher oligosaccharides contained in fractions **II** and **III**. It has been proposed that oxidative depolymerisation of heparin (Vismara et al., 2007) generates N-acetylglucosaminic acid. Recently, this acid was identified as one of the products of oxidative depolymerisation of heparin by potassium permanganate (Beccati et al., 2010). The authors suggested oxidation of the reducing end monosaccharide as the mechanism for its formation. Such behavior is not observed for the reducing end IdoA, which we found to be fully degraded. The GalNAc4S residue therefore appears to be more resistant to radical attack during the depolymerisation of DS, presumably protected by the NAc and a sulfate group at C-4, leading only to ring opening.

Investigation of the Fenton depolymerisation of heparin has showed spectroscopic evidence for the existence of partial (ketone) and fully oxidized (carboxylic acids) moieties, possibly also dicarboxylated structures either as reaction intermediates (Vismara et al., 2010) or as parts of the final products (Vismara et al., 2007, 2010). Carbonyl carbons were detected in the HMBC spectra in addition to those of the uronic acid and the hexosamine. We have not observed any signals in the ketone carbonyl region of the spectra (>200 ppm) of the depolymerised DS, however, the HMBC spectra of fraction **I** contained additional cross peaks (data not shown) in the carboxylic acid/ester region. It is, therefore, likely that minor species containing additional carboxyl groups are generated by the Fenton-type depolymerisation of DS.

The limiting experiment of our NMR methodology is the long-range proton-carbon correlation. The relaxation of coherences during the long evolution interval of the HMBC pulse sequence, together with a mixed phase of cross peaks, means that HMBC spectra of sufficient quality can only be obtained for smaller oligosaccharides – hence our emphasis on the analysis of the low molecular fractions. Nevertheless, once any unusual compounds and their $^{1}H$ and $^{13}C$ chemical shifts have been characterised by this methodology, sensitive methods such as 2D $^{1}H$,$^{13}C$ HSQC can be used to identify such structures in more complex mixtures containing larger oligosaccharides.

## 5. Conclusions

We can conclude that the $Cu^{2+}$ catalyzed Fenton degradation of DS proceeds in a similar manner to that of the depolymerisation of heparin. The differences between the two polymers, such as the nature of the hexosamine, its anomeric configuration and differences in glycosidic linkages and sulfation patterns, do not affect the depolymerisation process. Analysis of the low molecular fraction obtained by Fenton-type depolymerisation of DS in the presence of $Cu^{2+}$ yielded oligosaccharides containing the native DS sequence with GalNAc4S as the reducing end residue. In addition, we have identified a trisaccharide in which the reducing end GalNAc4S was oxidized to form N-acetylgalactosaminic acid. The existence of native species produced by this method holds promise for use in the fractionation of DS for biological applications and also for the generation of oligosaccharides for structure determination of unknown DS species. High sulfation levels do not necessarily stop the radical depolymerisation of GAGs as exemplified by Fenton depolymerisation of fucosylated 4,6 sulfated chondroitin sulfate isolated from a sea cucumber (Wu, Xu, Zhao, Kang, & Ding, 2010a, 2010b). Nevertheless, further work is needed to assess the specificity and efficiency of bond cleavages in oversulfated GAGs. Our work also demonstrates that a combination of several heterocorrelated NMR experiments at high magnetic fields can lead to a detailed structural analysis of related oligosaccharides as part of complex mixtures.

## Acknowledgements

This work was supported by ScotChem SPIRIT studentship to C. Panagos in association with GlycoMar Ltd.

## References

Beccati, D., Roy, S., Yu, F., Gunay, N. S., Capila, I., Lech, M., et al. (2010). Identification of a novel structure in heparin generated by potassium permanganate oxidation. *Carbohydrate Polymers*, *82*, 699–705.

Cássaro, C. M. & Dietrich, C. P. (1977). Distribution of sulfated mucopolysaccharides in invertebrates. *The Journal of Biological Chemistry*, *252*, 2254–2261.

Castelli, R., Porro, F. & Tarsia, P. (2004). The heparins and cancer: Review of clinical trials and biological properties. *Vascular Medicine*, *9*, 205–213.

Chen, S. G., Xue, C. H., Yin, L. A., Tang, Q. J., Yu, G. L. & Chai, W. G. (2011). Comparison of structures and anticoagulant activities of fucosylated chondroitin sulfates from different sea cucumbers. *Carbohydrate Polymers*, *83*, 688–696.

Cicero, D. O., Barbato, G. & Bazzo, R. (2001). Sensitivity enhancement of a two-dimensional experiment for the measurement of heteronuclear long-range coupling constants, by a new scheme of coherence selection by gradients. *Journal of Magnetic Resonance*, *148*, 209–213.

Comper, W. D & Laurent, T. C. (1978). Physiological function of connective tissue polysaccharides. *Physiological Reviews*, *58*, 255–315.

Fabris, F., Luzzatto, G., Stefani, P. M., Girolami, B., Cella, G. & Girolami, A. (2000). Heparin-induced thrombocytopenia. *Haematologica*, *85*, 72–81.

Guerrini, M., Naggi, A., Guglieri, S., Santarsiero, R. & Torri, G. (2005). Complex glycosaminoglycans: Profiling substitution patterns by two-dimensional nuclear magnetic resonance spectroscopy. *Analytical Biochemistry*, *337*, 35–47.

Imberty, A., Lortat-Jacob, H. & Pérez, S. (2007). Structural view of glycosaminoglycan-protein interactions. *Carbohydrate Research*, *342*, 430–439.

Legnani, C., Palareti, G., Biagi, R., Ludovici, S., Maggiore, L., Milani, M. R., et al. (1994). Acute and chronic effects of a new low molecular weight dermatan sulphate (Desmin 370) on blood coagulation and fibrinolysis in healthy subjects. *European Journal of Clinical Pharmacology*, *47*, 247–252.

Liaw, P. C., Becker, D. L., Stafford, A. R., Fredenburgh, J. C. & Weitz, J. I. (2001). Molecular basis for the susceptibility of fibrin-bound thrombin to inactivation by heparin cofactor ii in the presence of dermatan sulfate but not heparin. *The Journal of Biological Chemistry*, *276*, 20959–20965.

Lindahl, U. & Höök, M. (1978). Glycosaminoglycans and their binding to biological macromolecules. *The Annual Review of Biochemistry*, *47*, 385–417.

Linhardt, R. J. & Gunay, N. S. (1999). Production and chemical processing of low molecular weight heparins. *Seminars in Thrombosis and Hemostasis*, *3*(25 (Suppl.)), 5–16.

Linhardt, R. J. & Hileman, R. E. (1995). Dermatan sulfate as a potential therapeutic agent. *General Pharmacology*, *26*, 443–451.

Linhardt, R. J., Loganathan, D., al-Hakim, A., Wang, H. M., Walenga, J. M., Hoppensteadt, D., et al. (1990). Oligosaccharide mapping of low molecular weight

heparins: Structure and activity differences. *The Journal of Medicinal Chemistry*, *33*, 1639–1645.

Mascellani, G., Liverani, L., Parma, B., Bergonzini, G. L. & Bianchini, P. (1996). Active site for heparin cofactor II in low molecular mass dermatan sulfate. Contribution to the antithrombotic activity of fractions with high affinity for heparin cofactor II. *Thrombosis Research*, *84*, 21–32.

Mathews, M. B. (1975). Connective tissue. Macromolecular structure and evolution. *Molecular Biology, Biochemistry & Biophysics*, 1–318.

Medeiros, G. F., Mendes, A., Castro, R. A., Baú, E. C., Nader, H. B. & Dietrich, C. P. (2000). Distribution of sulfated glycosaminoglycans in the animal kingdom: Widespread occurrence of heparin-like compounds in invertebrates. *Biochimica et Biophysica Acta*, *1475*, 287–294.

Mourão, P. A., Pereira, M. S., Pavão, M. S., Mulloy, B., Tollefsen, D. M., Mowinckel, M. C., et al. (1996). Structure and anticoagulant activity of a fucosylated chondroitin sulfate from echinoderm. Sulfated fucose branches on the polysaccharide account for its high anticoagulant action. *The Journal of Biological Chemistry*, *271*, 23973–23984.

Nagasawa, K., Uchiyama, H., Sato, N. & Hatano, A. (1992). Chemical change involved in the oxidative–reductive depolymerization of heparin. *Carbohydrate Research*, *236*, 165–180.

Ofman, D., Slim, G. C., Watt, D. K. & Yorke, S. C. (1997). Free radical induced oxidative depolymerisation of chondroitin sulphate and dermatan sulphate. *Carbohydrate Polymers*, *33*, 47–56.

Pavão, M. S., Mourão, P. A., Mulloy, B. & Tollefsen, D. M. (1995). A unique dermatan sulfate-like glycosaminoglycan from ascidian. Its structure and the effect of its unusual sulfation pattern on anticoagulant activity. *The Journal of Biological Chemistry*, *270*, 31027–31036.

Uchiyama, H., Dobashi, Y., Ohkouchi, K. & Nagasawa, K. (1990). Chemical change involved in the oxidative reductive depolymerization of hyaluronic acid. *The Journal of Biological Chemistry*, *265*, 7753–7759.

Vieira, R. P., Mulloy, B. & Mourão, P. A. (1991). Structure of a fucose-branched chondroitin sulfate from sea cucumber. Evidence for the presence of 3-O-sulfo-beta-D-glucuronosyl residues. *The Journal of Biological Chemistry*, *266*, 13530–13536.

Vismara, E., Pierini, M., Guglieri, S., Liverani, L., Mascellani, G. & Torri, G. (2007). Structural modification induced in heparin by a Fenton-type depolymerization process. *Seminars in Thrombosis and Hemostasis*, *33*, 466–477.

Vismara, E., Pierini, M., Mascellani, G., Liverani, L., Lima, M., Guerrini, M., et al. (2010). Low-molecular-weight heparin from $Cu^{2+}$ and $Fe^{2+}$ Fenton type depolymerisation processes. *Journal of Thrombosis and Haemostasis*, *103*, 613–622.

Volpi, N. (2010). Dermatan sulfate: Recent structural and activity data. *Carbohydrate Polymers*, *82*, 233–239.

Volpi, N., Mascellani, G. & Bianchini, P. (1992). Low molecular weight heparins (5 kDa) and oligoheparins (2 kDa) produced by gel permeation enrichment or radical process: Comparison of structures and physicochemical and biological properties. *Analytical Biochemistry*, *200*, 100–107.

Wu, M. Y., Xu, S. M., Zhao, J. H., Kang, H. & Ding, H. (2010a). Free-radical depolymerization of glycosaminoglycan from sea cucumber *Thelenata ananas* by hydrogen peroxide and copper ions. *Carbohydrate Polymers*, *80*, 1116–1124.

Wu, M. Y., Xu, S. M., Zhao, J. H., Kang, H. & Ding, H. (2010b). Preparation and characterization of molecular weight fractions of glycosaminoglycan from sea cucumber *Thelenata ananas* using free radical depolymerization. *Carbohydrate Research*, *345*, 649–655.